MOLECULAR AND CELLULAR BIOLOGY, Jan. 2010, p. 260–272 Vol. 30, No. 1
0270-7306/10/$12.00 doi:10.1128/MCB.00645-09

Friend of Prmt1, a Novel Chromatin Target of Protein Arginine Methyltransferases▽

Thamar Bryn van Dijk,[1] Nynke Gillemans,[1] Claudia Stein,[2] Pavlos Fanis,[1] Jeroen Demmers,[3] Mariëtte van de Corput,[1] Jeroen Essers,[4] Frank Grosveld,[1] Uta-Maria Bauer,[2] and Sjaak Philipsen[1]*

Department of Cell Biology, Erasmus MC, 3015 GE Rotterdam, The Netherlands[1]; Institute for Molecular Biology and Tumor Research, Philipps University Marburg, 35032 Marburg, Germany[2]; Netherlands Proteomics Centre, Erasmus MC, 3015 GE Rotterdam, The Netherlands[3]; and Department of Genetics, Erasmus MC, 3015 GE Rotterdam, The Netherlands[4]

Received 19 May 2009/Returned for modification 19 June 2009/Accepted 14 October 2009

We describe the isolation and characterization of Friend of Prmt1 (Fop), a novel chromatin target of protein arginine methyltransferases. Human Fop is encoded by *C1orf77*, a gene of previously unknown function. We show that Fop is tightly associated with chromatin, and that it is modified by both asymmetric and symmetric arginine methylation in vivo. Furthermore, Fop plays an important role in the ligand-dependent activation of estrogen receptor target genes, including *TFF1* (*pS2*). Fop depletion results in an almost complete block of estradiol-induced promoter occupancy by the estrogen receptor. Our data indicate that Fop recruitment to the promoter is an early critical event in the activation of estradiol-dependent transcription.

Arginine methylation is a widespread posttranslational modification in eukaryotic cells that is catalyzed by a family of enzymes called protein arginine methyltransferases (Prmts). Prmts use *S*-adenosyl-L-methionine (SAM) as a donor to transfer methyl groups to the side-chain nitrogens of arginine residues. To date, nine Prmts have been identified in humans, and they have been subdivided into two major classes. Type I enzymes (Prmt1, Prmt3, Prmt4, Prmt6, and Prmt8) promote the formation of asymmetrical ω-N^G,N^G-dimethylated arginines (aDMA), and type II enzymes (Prmt5 and Prmt7) form symmetrical ω-N^G,N'^G-dimethylated arginines (sDMA). ω-N^G-monomethylarginine (MMA) is thought to be an intermediate formed by both enzyme types. So far, the methyltransferase activity of Prmt2 and Prmt9 has not been demonstrated formally (6, 36). Although methylation does not change the overall charge of an arginine residue, it modulates intermolecular interactions by increasing steric hindrance and hydrophobicity and decreasing hydrogen-bonding capacity. Furthermore, methylation protects the reactive guanidino groups of arginine residues against inappropriate modification by dicarbonyl reagents (15).

Prmt1 is ubiquitously expressed and is the source of the predominant Prmt activity in mammalian cells. Although Prmt1-deficient embryonic stem cell lines are viable, Prmt1 knockout mice die at around the onset of gastrulation, which is consistent with a fundamental and nonredundant function (38). The majority of previously identified Prmt1 substrates are nucleic acid binding proteins that play a role in RNA processing, DNA repair, signal transduction, and transcription (6, 34). How Prmt1 recognizes its specific substrates, and to what degree this is regulated by additional factors, is only partially understood. Prmt1 has a high affinity for glycine-arginine-rich (GAR) regions, and the majority of identified methylated arginines are located within such domains (6). The crystal structure of Prmt1 in complex with a GAR peptide reveals three different binding channels for these motifs (51). GAR regions are a common feature of many RNA-binding proteins (RBPs), including the heterogeneous ribonucleoproteins (hnRNPs). These proteins play roles in mRNA processing and transport and contain up to 65% of total nuclear DMA (8, 26). Although the arginines in these regions have been recognized as key residues in RNA-protein interactions, it remains to be determined whether methylation has a profound effect on protein-RNA interactions. In contrast, a role for arginine methylation in regulating protein-protein interactions is well documented. The methylation of the yeast hnRNPs Npl3p and Hrp1p and the RBPs Sam68 and RNA helicase A is critical for their proper cellular localization (42, 50). The methylation of Sam68 regulates binding to SH3 domain-containing proteins, while binding to WW domains is unaffected (7). Other interactions controlled by DMA include transcription factor complexes, such as the binding of Nip45 to Nfat and the binding of Cbp/p300 to Creb (30, 49).

Another mechanism of substrate recognition is regulated via controlled recruitment. For example, Prmts are recruited to promoters and other regulatory elements to control gene expression by the methylation of histones and components of the transcription machinery (36). The recruitment of Prmt1 by nuclear hormone receptors and the transcription factors p53, YY1/Drbp76, and upstream stimulatory factor 1 (Usf1) results in the local methylation of histone H4 at R3 (1, 19, 39, 48). This modification is critical for subsequent histone acetylation and further activation events (20).

Little is known about the regulation of the enzymatic activity of Prmt1. As most target proteins appear to be methylated entirely at any given time, Prmt1 is considered to be a consti-

* Corresponding author. Mailing address: Erasmus MC, Department of Cell Biology, Rm Ee720a, Molewaterplein 50, 3015 GE Rotterdam, The Netherlands. Phone: 31-107044282. Fax: 31-104089468. E-mail: j.philipsen@erasmusmc.nl.

▽ Published ahead of print on 26 October 2009.

tutively active enzyme. Prmt1 activity is abolished when dimerization is prevented, and it has been suggested that Prmt1 is catalytically active only in the form of oligomers (24, 51). In all cell lines tested, Prmt1 is a component of a 250- to 400-kDa complex both in the cytoplasm and in the nucleus. It is unclear whether additional proteins are a constitutive component of this complex or whether it reflects a large Prmt1 polymer. Furthermore, only a limited number of Prmt1-interacting proteins have been described to affect Prmt1 activity under certain conditions. CCR4-associated factor 1 (Caf1) and the related proteins B-cell translocation gene 1 (Btg1) and Btg2/Tis21 bind Prmt1 and stimulate its activity toward selected substrates, while protein phosphatase 2A (Pp2a) has an inhibitory effect (13, 25, 40).

The identification and characterization of Prmt1-interacting proteins is critical for further understanding the role of Prmt1 in different cellular processes and may answer questions regarding the regulation of Prmt1 activity and specificity. Thus far, Prmt1 substrates and Prmt1-interacting proteins have been identified through candidate approaches, serendipitous discovery, in vitro substrate screens, and proteomic strategies that identify proteins with methylated arginines (10, 33, 46). Here, we describe the single-step isolation of Prmt1-associating proteins using a biotinylation-proteomics approach and the characterization of a novel Prmt1-interacting protein, which we termed Friend of Prmt1 (Fop).

MATERIALS AND METHODS

Constructs and cells. The coding sequence of Prmt1 (isoform 1) was amplified from mouse erythroblast cDNA by PCR using Expand (Roche), cloned into pMT2_HA and pMT2_myc (22) using SalI and NotI, and verified by sequencing. After the introduction of the 23-amino-acid (aa) biotinylation tag (designated Bio-tag), HA_bio_Prmt1 was subcloned into the erythroid expression vector pEV-neo (32) and electroporated into mouse erythroleukemic (MEL) cells expressing the BirA biotin ligase (12). The cDNA of Fop was obtained from RZPD/imaGenes (clone IRAKp961L04114Q2; Berlin, Germany). The first 25 aa were introduced using SalI/HindIII after subcloning the 930-bp HindIII/EcoRV fragment into pBluescript (Stratagene). Full-length Fop was cloned into pMT2_HA using SalI and EcoRI sites. Glutathione *S*-transferase–Fop (GST-Fop) fusion constructs were generated by cloning PCR fragments into pGEX3X (Pharmacia). Green fluorescent protein (GFP) and Cherry were cloned in frame at the N terminus of Fop and Prmt1, respectively. MEL, 293T, U2OS, and MCF7 cells were grown in Dulbecco's modified Eagle medium (DMEM; Life Technologies) supplemented with 10% fetal calf serum (FCS). Before hormone treatment, MCF7 cells were grown for 3 to 4 days in phenol red-free DMEM supplemented with 5% charcoal-dextran-stripped FCS after the addition of 200 nM 17β-estradiol (E2; Sigma) for the indicated times.

Size fractionation. The size fractionation of protein complexes was carried out on an AKTA fast-performance liquid chromatography apparatus with a Superose 6 10/30 column (Amersham Biosciences). Fractions were precipitated with trichloroacetic acid and analyzed by Western blotting.

Transient transfection, immunoprecipitation, and Western blot analysis. The transfection of 293T cells, immunoprecipitation, GST pull downs, and Western blot analysis were performed as described previously (45). Membranes were blocked in 0.6% bovine serum albumin (BSA), incubated with the appropriate antibodies, and developed with the use of enhanced chemiluminescence (NEN) or by using the Odyssey infrared imaging system (Li-Cor Biosciences). The following primary antibodies were used: Prmt1 (07-404), Prmt5 (07-4051), H4R3me2 (07-213), AcH4 (06-598), H3K27me3 (07-449), Asym24 (07-414), and Sym10 (07-412) were from Upstate; hemagglutinin (HA) (monoclonal F7; sc-7392), HA (polyclonal Y11; sc-805), Myc (sc-40), actin (sc-1616), Shc (sc-967), and lamin B (sc-6216) were from Santa Cruz; and LSD (ab18036), H3K9me2 (ab1220), and H3 (ab1791) were from Abcam. Rat monoclonal antibodies against the N and C termini of Fop (KT59 recognizing aa 1 to 90 and KT64 recognizing aa 206 to 249, respectively) were generated by Absea Biotechnology Ltd. (Beijing, China). Additionally, polyclonal antibodies were raised in rabbits using the same epitopes. Cellular fractionation was performed as described previously (37). Subcellular fractionation (cytoplasm, nucleoplasm, chromatin, and nuclear matrix) was performed as described previously (31).

Cellular extracts and mass spectrometry. Procedures involving biotinylated proteins were performed as described previously, with minor modifications (12). Cytoplasmic and nuclear extracts were generated using the method of Andrews and Faller from 5×10^8 MEL cells (2). Tryptic digestion was performed on paramagnetic streptavidin beads. Mass spectrometry (MS) was performed as described previously (3). Nanoflow liquid chromatography (LC)-MS/MS was performed on an 1100 series capillary LC system (Agilent Technologies) coupled to an LTQ-Orbitrap mass spectrometer (Thermo) operating in positive mode and equipped with a nanospray source. Peptide mixtures were trapped on a ReproSil C_{18} reversed-phase column (column dimensions, 1.5 cm by 100 μm; packed in-house; Maisch GmbH) at a flow rate of 8 μl/min. Peptide separation was performed on a ReproSil C_{18} reversed-phase column (column dimensions, 15 cm by 50 μm; packed in-house; Maisch GmbH) using a linear gradient from 0 to 80% B (A, 0.1% formic acid; B, 80% [vol/vol] acetonitrile, 0.1% formic acid) for 70 min and at a constant flow rate of 200 nl/min using a splitter. The column eluent was directly sprayed into the electrospray ionization (ESI) source of the mass spectrometer. Mass spectra were acquired in continuum mode; the fragmentation of the peptides was performed in data-dependent mode. Peak lists were automatically created from raw data files using the Mascot Distiller software (version 2.1; MatrixScience). The Mascot search algorithm (version 2.2, MatrixScience) was used for searching against the NCBInr database (release 20090430; total number of sequences, 8,483,808). The peptide tolerance typically was set to 10 ppm, and the fragment ion tolerance was set to 0.8 Da. A maximum number of two missed cleavages by trypsin were allowed, and carbamidomethylated cysteine and oxidized methionine were set as fixed and variable modifications, respectively. The Mascot score cutoff value for a positive protein hit was set to 75. Typical contaminants, which also are present in purifications using BirA-only MEL cell extracts, were omitted from the table (12).

Lentivirus-mediated knockdown and siRNAs. After being subcloned into pSuper (11), the H1 promoter and short hairpin RNA (shRNA) coding sequences against Prmt1 (GATTGTCAAAGCCAACAAG) and Fop (GGAGCA GCTGGACAACCAA) were cloned into a modified pRRLsin.sPPT.CMV. GFP.Wpre lentiviral vector (16). Lentivirus was produced by the transient transfection of 293T cells according to standard protocols (52). Knockdowns in MCF7 were performed using short interfering RNA (siRNA) transfection as described previously (47). The sequences of siRNA against Fop (siFop) are 5′-GGAGCA GCUGGACAACCAA-3′, 5′-GUUAGUCAACACAUCUGUAAA-3′, and 5′-G ACUCUUGUUAGUCAACACAU-3′ (sense strand; Genepharma, Shanghai, China).

Confocal imaging. For confocal imaging, cells were spotted on poly-prep slides (Sigma), fixed with 4% paraformaldehyde in phosphate-buffered saline (PBS), permeabilized with 0.1% Triton X-100, and blocked in 1% BSA–0.05% Tween 20 in PBS. Primary antibody incubation was performed in blocking solution for 16 h at 4°C. Cells were imaged using a Meta 510 confocal laser-scanning microscope (Meta LSM510; Zeiss) using the AIM software provided. Images were recorded as an 8-bit image stack of 512 by 512 pixels with a voxel size of 47 by 47 by 250 nm of a 4× line average. The point spread function was determined by scanning green fluorescent beads with a diameter of 100 nm (Duke Scientific). The chromatic shift was determined by scanning multicolored fluorescent beads with a diameter of 500 nm (TetraSpeck beads; Invitrogen). The empirically obtained point spread function (PSF) was used for deconvolving the image stacks with the classic maximum of likelihood algorithm that is implemented in the Huygens deconvolution, visualization, analysis, and archiving software package 3.0 for Linux (Scientific Volume Imaging). After deconvolution, the image stack was corrected for chromatic shift. Fluorescence recovery after photobleaching and fluorescence loss in photobleaching (FRAP/FLIP) experiments were performed as described previously (14).

RT, ChIP, and QPCR. Reverse transcription (RT) and chromatin immunoprecipitation (ChIP) were performed as previously described (47). For RT-quantitative PCR (RT-QPCR), GAPDH gene transcription was used as a reference for normalization. The following primers were used: GAPDH, 5′-AGC CACATCGCTCAGACAC-3′ (forward) and 5′-GCCCAATACGACCAAATC C-3′ (reverse); pS2, 5′-GCCTTTGGAGCAGAGAGGA-3′ (forward) and 5′-T AAAACAGTGGCTCCTGGCG-3′ (reverse); lactoferrin, 5′-TAAGGTGGAA CGCCTGAAAC-3′ (forward) and 5′-CCATTTCTCCCAAATTTAGCC-3′ (reverse); and transforming growth factor alpha (TGF-α), 5′-TGCTGCCACTC AGAAACAGT-3′ (forward) and 5′-ATCTGCCACAGTCCACCTG-3′ (reverse). For ChIP-QPCR, immunoprecipitated chromatin was amplified using the following primers: pS2 gene promoter, 5′-GTTGTCACGGCCAAGCCTTTT-3′ (forward) and 5′-AGGATTTGCTGATAGACAGAGACGAC-3′ (reverse); and

GAPDH gene promoter, 5′-CCATCTCAGTCGTTCCCAAAGTCC-3′ (forward) and 5′-GATGGGAGGTGATCGGTGCT-3′ (reverse). The ChIP results were quantified as recently described (21).

RESULTS

Identification of Prmt1-associated proteins by biotinylation tagging and MS. Tagged Prmt1 (HA_bio_Prmt1) was generated by fusing an HA epitope and a short (23-aa) Bio-tag to its N terminus. The Bio-tag is efficiently biotinylated by the bacterial BirA biotin ligase, which is coexpressed in stably transfected MEL cells (12). HA_bio_Prmt1 was expressed below endogenous levels to reduce the likelihood that nonphysiological interactions would be identified. Biotinylated Prmt1 was efficiently recovered from MEL extracts with magnetic streptavidin beads and was associated with endogenous Prmt1 in both the cytoplasm and the nucleus (Fig. 1A). Size fractionation experiments showed that HA_bio_Prmt1 behaved similarly to endogenous Prmt1, eluting in fractions with a molecular mass range of 250 to 400 kDa (44) (Fig. 1B). Complexes with a molecular mass of more than 1 MDa were detected exclusively in the nuclear fraction. In contrast, Prmt1 with a C-terminal HA_Bio-tag appeared to be monomeric (42 kDa [data not shown]). These experiments show that HA_bio_Prmt1 is faithfully incorporated into oligomeric complexes. Prmt1-associating proteins were identified by streptavidin pull down followed by nanoflow LC-MS/MS and were compared to samples from cells expressing BirA alone. Putative Prmt1-interacting proteins identified in two independent HA_bio_Prmt1 pull downs are listed in Fig. 1C. The candidates are predominantly RBPs involved in RNA processing (Rbmxrt/hnRNPG, hnRNPU, and Lsm14a), RNA stability (Serbp1), RNA export (Refbp2), translation (Msy4), and ribosome synthesis (Nol5a). All proteins contain GAR domains, suggesting that these proteins are direct targets for Prmt activity. Indeed, the methylation of hnRNPs, including Rbmxrt/hnRNPG and hnRNPU, is well documented, while members of the SM/LSm family are previously identified targets of Prmt5 (9, 26). Multiple known Prmt1 targets/interacting proteins, including additional hnRNPs, U5 snRNP components, Sam68, and fibrillarin, also were detected, but these abundant proteins also were found in the BirA-only control samples as observed previously (12).

A newly identified putative Prmt1-interacting protein is encoded by the homolog of the human *C1orf77* gene. The protein has not been characterized previously, and as it interacts with Prmt1 (see Fig. 3), we named it Friend of Prmt1 (Fop). Fop has an expected molecular mass of 27 kDa and is highly conserved in all vertebrates (Fig. 1D), while no orthologs could be identified in yeast, worms, and flies. The protein has no known conserved domains, but its central sequence consists of a GAR domain that contains 26 RG/GR repeats, while the C terminus harbors a duplication of the sequence LDXXLDAYM (where X is any amino acid). Furthermore, we note that the sequence of the GAR domain shows more variation (70% conservation) than those of the N and C termini (80% conservation for both).

Intracellular localization and expression pattern of Fop. For the further characterization of the protein, monoclonal antibodies were raised against the N and C termini of Fop. Both clone KT59 (specific for the N terminus) and KT64 (specific for the C terminus) recognized a protein running at the expected molecular mass of 27 kDa (Fig. 2A) and additional proteins of 23 and 25 kDa. These proteins were not detected in cells expressing an shRNA against Fop, suggesting that they represent full-length Fop and smaller isoforms, respectively. It is possible that the 23- or 25-kDa isoform represents Fop_S, an isoform lacking the first 25 aa at the N terminus (Fig. 1D). In immunoprecipitation (IP) experiments, the different isoforms of Fop were purified by both KT59 and KT64, although the 25-kDa isoform is masked by the immunoglobulin G (IgG) light chain of KT59 (Fig. 2B). Full-length Fop appeared as a doublet, indicating that it is a target for posttranslational modifications. Analysis by confocal microscopy showed that Fop is a nuclear protein localized to regions with low levels of DAPI, with a punctate/speckle-like distribution (Fig. 2C; also see Fig. 5). We next determined the expression of Fop in embryonic day 16.5 mouse embryos. We find that Fop has a wide but not ubiquitous expression pattern (Fig. 2D). Tissues expressing Fop include the heart, lungs, gut, kidney, submandibular gland, thymus, follicles of the vibrissae, muscle, brown fat, and neuronal cells, including brain, olfactory epithelium, and dorsal root ganglia (Fig. 2D). Identical results were obtained with KT59 (not shown).

Fop is a novel Prm1-interacting protein. To validate the interaction between Prmt1 and Fop, we transiently cotransfected HA_Fop with wild-type Myc_Prmt1 or the enzymatic inactive mutant Myc_Prmt1_E171Q in 293T cells. Wild-type and mutant Myc_Prmt1, as well as endogenous Prmt1, are efficiently recovered in HA_Fop IPs, confirming the interaction between Prmt1 and the Fop protein (Fig. 3A). Cotransfection with wild-type Prmt1 resulted in a slightly slower migration of HA_Fop, suggesting that Fop is modified by Prmt1 (Fig. 3A). Incubation with an antibody that specifically recognizes asymmetrically methylated arginines (Asym24) shows that Fop is indeed an aDMA-containing protein. The interaction between endogenous proteins then was studied using monoclonal antibodies KT59 and KT64.

Figure 3B shows that Prmt1 is detected in Fop purifications (left) and that Fop coimmunoprecipitates with Prmt1 (right), confirming that the endogenous proteins interact.

To identify the region of Fop that interacts with Prmt1, we generated a panel of Fop deletion mutants fused to the C terminus of GST. The deletion series included two potential isoforms (Fop_L and Fop_S, which lack the first 25 aa) (Fig. 1D) and progressive N- and C-terminal deletions (Fig. 3C). The GST_Fop fusions were incubated with whole-cell extracts from MEL cells as a source of Prmt1. These results were obtained under stringent washing conditions (radioimmunoprecipitation assay buffer containing 0.1% sodium dodecyl sulfate, 0.5% deoxycholate, 1% NP-40), indicating that the observed interactions are specific. The C-terminal half of the central GAR domain (from R153 to G205) was identified as the major interaction site, which is in line with previous observations that Prmt1 has a high affinity for GAR sequences (6, 34). A second, weaker binding domain was found within the first 90 aa in the N terminus (Fig. 3C and 4D).

Fop is methylated by Prmt1 and Prmt5 in vitro and in vivo. To investigate whether Fop is a target of Prmt activity, we performed in vitro methylation assays using purified GST_Prmt1,

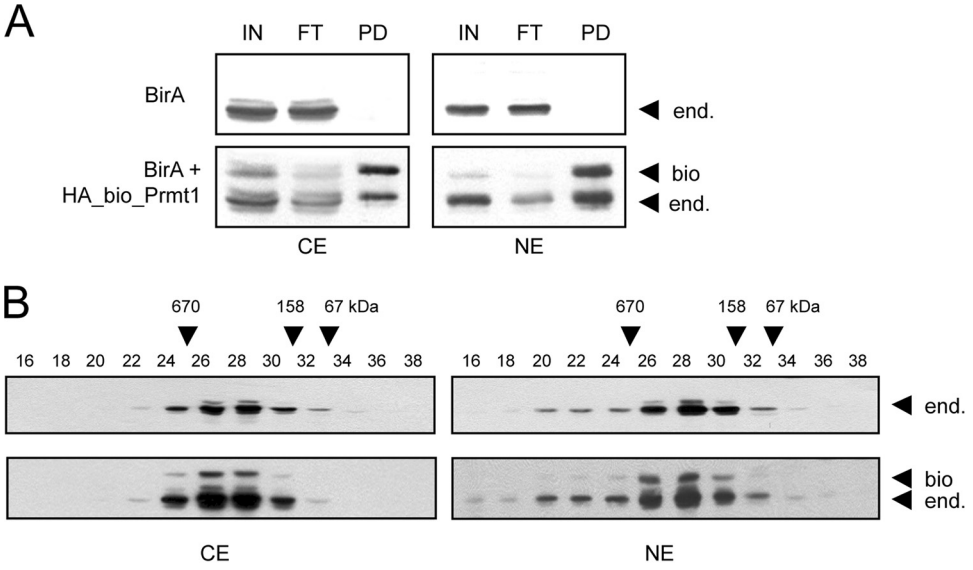

C

		experiment 1		experiment 2	
Description	Gene ID	% cover.	pept. uniq.	% cover.	pept. uniq.
Prmt1	9790109	39,7	14	39,7	14
Rbmxrt	1327760	24,7	9	22,7	8
Msy4	7385223	19,1	6	24,4	8
C1orf77 homolog	54036077	23,2	4	23,2	4
hnRNPU	7949051	4,6	3	7,1	6
Serbp1	20988551	7,9	2	3,9	1
Refbp2	68534069	12,9	2	23,9	3
Nol5a	12805509	4,9	1	7,8	3
Lsm14a	21618722	6	2	6	2

D

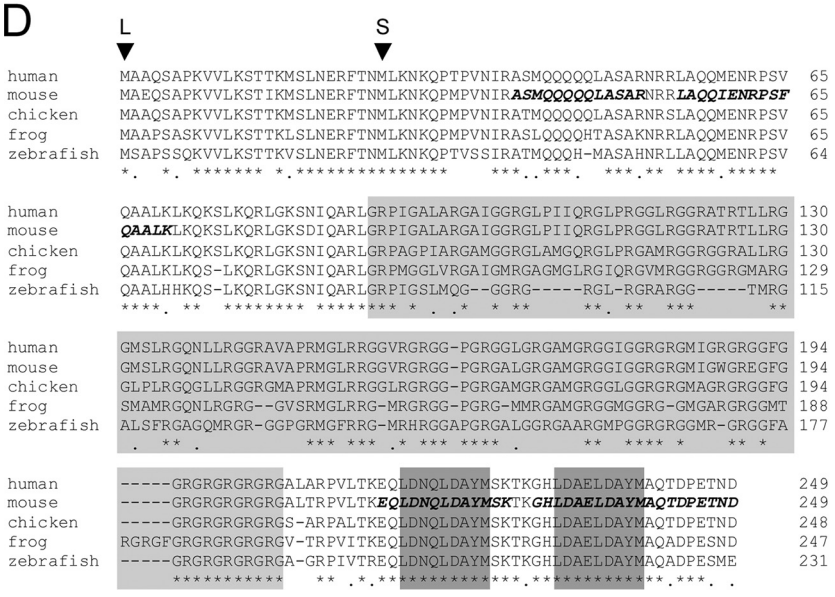

FIG. 1. Biotinylation of Prmt1 in MEL cells. (A) Biotinylated Prmt1 (bio) is pulled down from cytoplasmic (CE) and nuclear extracts (NE) of MEL cells expressing the BirA biotin ligase. Since Prmt1 forms oligomers in vivo, endogenous (end.) Prmt1 copurifies with HA_bio_Prmt1 in streptavidin pulldowns. IN, input; FT, flowthrough; PD, pull down. (B) Size fractionation profiles of Prmt1; the profile of tagged Prmt1 (bio) closely follows that of endogenous Prmt1 (end.) in cytoplasmic (CE) and nuclear extracts (NE). Molecular mass markers are indicated at the top. The top panels indicate BirA control cells. (C) Prmt1-interacting proteins identified by MS. Gene identities (from NCBI), percent coverage (% cover.), and numbers of unique peptides (pept. uniq.) identified are indicated. (D) Alignment of predicted full-length amino acid sequences of vertebrate Fop homologs (Fop_L). Transcripts lacking the first coding exon are found in human and mouse only and start at M26 (Fop_S). The GAR domain (light gray) and C-terminal duplication (dark gray) are indicated. Identified tryptic peptides are indicated in boldface and italics.

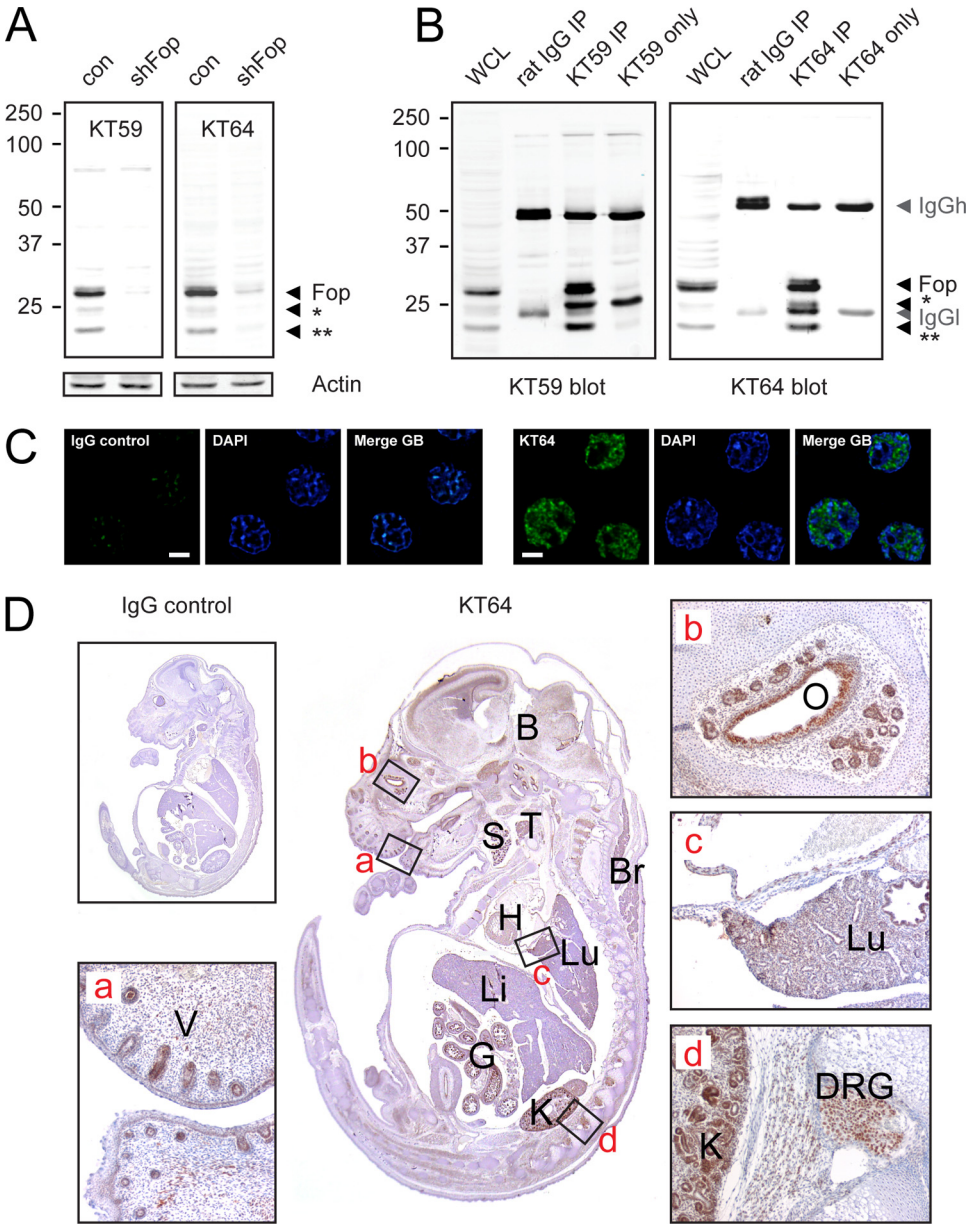

FIG. 2. Intracellular localization and expression pattern of Fop. (A and B) A doublet of ~27 kDa and isoforms of ~25 and ~23 kDa (indicated by single and double asterisks, respectively) are recognized (A) and precipitated (B) by KT59, a monoclonal antibody raised against the N terminus of Fop (aa 1 to 90), and by KT64, raised against the C terminus (aa 206 to 249). The detection of these proteins is sharply diminished in lysates from cells expressing an shRNA against Fop (shFop). con, control; WCL, whole-cell lysate. (C) Confocal images showing that Fop localizes to regions in the nucleus with low levels of DAPI and displays a granulated/speckle-like distribution in MEL cells. GB, green and blue signals. (D) Sagittal paraffin sections of embryonic day 16.5 mouse embryos were incubated with rat IgG control and KT64, followed by peroxidase staining. B, brain; Br, brown fat; DRG, dorsal root ganglion; G, gut; H, heart; Li, liver; O, olfactory epithelium; S, submandibular gland; T, thymus; and V, follicles of vibrissae.

GST_Prmt4, GST_Prmt6, and immunoprecipitated Prmt5 in the presence of methyl-^{14}C-labeled SAM. Core histones served as a positive control (Fig. 4A and B, upper). We find that Prmt1 is the only type I enzyme tested that is able to methylate Fop (Fig. 4A, lower). In addition, Prmt5 can use Fop as a substrate (Fig. 4B, lower), opening the possibility that Fop contains symmetrically methylated arginines in vivo. To investigate this further, we performed the lentivirus-mediated knockdown of Prmt1 and Prmt5 in MEL cells. The reduction of the protein level of Prmt1 resulted in a dramatic shift of the migration pattern of Fop (Fig. 4C, upper), suggesting that Fop is heavily modified by Prmt1. To test this directly, endogenous Fop was immunoprecipitated from control cells and Prmt1 knockdown cells and stained with the Asym24 antibody. This revealed that the asymmetrical arginine methylation of Fop is severely reduced in the absence of Prmt1 (Fig. 4C, lower). This shows that (i) target arginines of Prmt1 in Fop are methylated in vivo, (ii) Prmt1 is the major type I enzyme that methylates

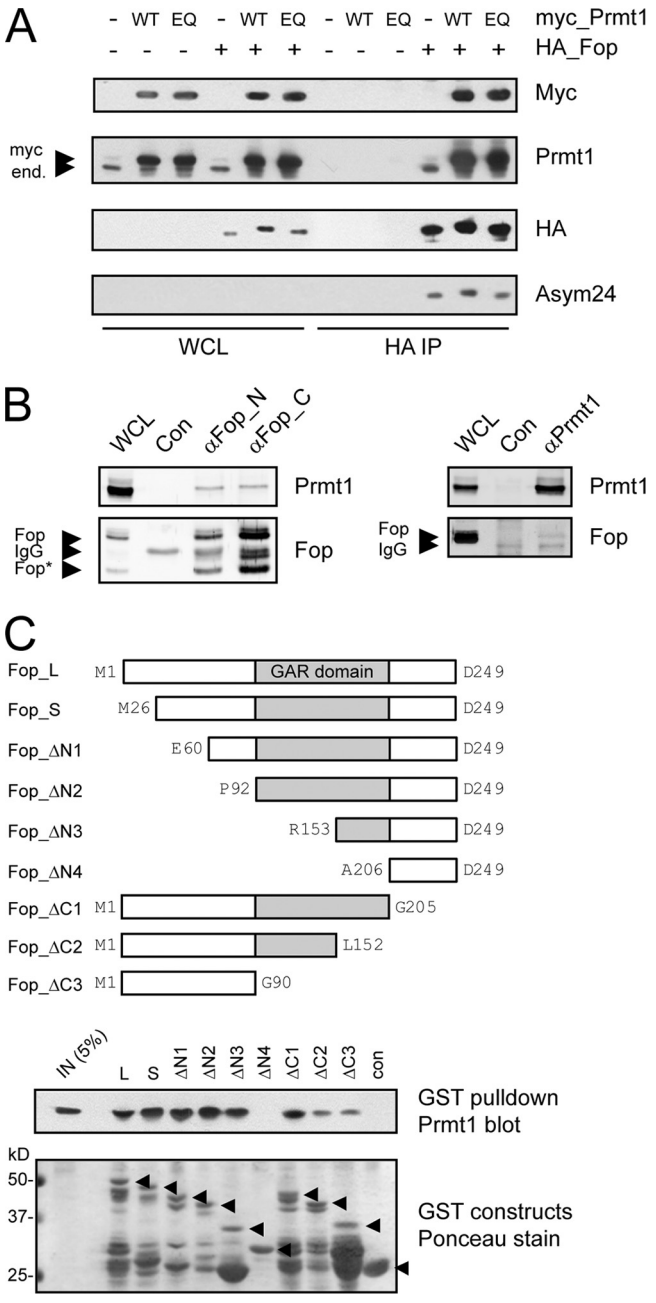

FIG. 3. Fop is a Prmt1-associating protein. (A) 293T cells were cotransfected with HA_Fop and wild-type Myc_Prmt1 (WT) or enzymatically inactive Myc_Prmt1_E171Q (EQ). HA_Fop was precipitated and blots were stained for Myc, Prmt1, HA, and an antibody recognizing asymmetrically methylated arginines (Asym24). Prmt1 binds and methylates HA_Fop. (B) Monoclonal antibodies specifically recognizing the N- and C-terminal domains of Fop confirm the interaction of endogenous Fop and Prmt1. The smaller isoform of Fop is indicated with an asterisk. (C) The upper panel shows a schematic representation of GST_Fop deletion constructs. The lower panels show GST constructs incubated with MEL extracts as a source of Prmt1. Western blot analysis identified two regions in Fop that mediate binding to Prmt1: the N-terminal 90 aa (Fop_ΔC3) and R153 to A206 (compare Fop_ΔC2 to Fop_ΔN3). Total protein staining served as a loading control (lower right). Arrowheads indicate full-length GST fusion proteins. WCL, whole-cell lysate; end., endogenous Prmt1; Fop_L, full-length Fop; Fop_S, isoform lacking the first 25 aa; con, GST only; IN, input MEL cell extract.

Fop in vivo, and (iii) the reduced mobility of Fop on sodium dodecyl sulfate-polyacrylamide gel electrophoresis correlates with the presence of aDMA residues.

Since Prmt5 can methylate Fop in vitro, we stained similar blots with antibodies specific for Prmt5 and symmetrically methylated arginines (Sym10). In control cells, the interaction between Fop and Prmt5 can be detected (Fig. 4C). However, much more Prmt5 is coimmunoprecipitated with HA-Fop in the absence of Prmt1, indicating that Prmt1 and Prmt5 compete for binding to Fop. In line with the binding of Prmt5 and the in vitro methylation experiments, sDMA residues are detected in Fop both in the presence and absence of Prmt1 (Fig. 4C). Interestingly, the increased binding of Prmt5 to Fop in the absence of Prmt1 does not result in the elevated symmetrical methylation of Fop. In contrast, the Sym10 staining is less in the Prmt1 knockdown, suggesting that Prmt1 positively affects the symmetric dimethylation of Fop. Partially knocking down Prmt5 did not reduce the Sym10 staining of Fop, although this did reduce the expression level of Fop to ~75% of that observed in control cells. It is unclear whether this is the result of incomplete Prmt5 depletion or that other type II Prmt enzymes can methylate Fop in vivo. This could not be tested, as a complete knockdown of Prmt5 resulted in cell death, as has been shown previously for transformed B cells (35). We conclude that Fop contains asymmetric and symmetric DMA residues in vivo, and that symmetric methylation partially depends on the presence of Prmt1.

To map the arginines that are methylated within the GAR, we generated internal deletion constructs that lacked either the N-terminal or the C-terminal half of the GAR or the entire GAR (ΔGR1, ΔGR2, and ΔGR3, respectively) (Fig. 4D). The binding of Prmt1 and Prmt5 (Fig. 4D, right) as well as the methylation status (Fig. 4D, left) are not reduced when the N-terminal half is deleted, indicating that the majority of methylated arginines is not in this region. In contrast, the methylation and Prmt binding of FopΔGR2 is undetectable (Prmt5) or greatly reduced (Prmt1). Hence, the major Prmt interaction surface and methylation sites appear to overlap. Consistently with the interaction mapping, FopΔGR2 and FopΔGR3 still are able to recruit reduced levels of Prmt1 via the N-terminal domain (FopΔC3) (Fig. 3C).

Fop is a chromatin-associated protein. We next examined Fop and Prmt1 colocalization by confocal microscopy and fractionation experiments. Figure 5A shows that HA_Fop is a nuclear protein exclusively localized to regions with a low level of DAPI, with a punctate/speckle-like distribution (Fig. 5A), identically to endogenous Fop (Fig. 2C). Staining for endogenous Prmt1 revealed that, within the nucleus, Prmt1 also localizes to regions with a low level of DAPI, resulting in a high degree of colocalization with Fop (Fig. 5A). Compared to that of Fop, the distribution of Prmt1 is more diffuse. The distribution and pattern of Fop localization did not change in Prmt1-depleted cells (Fig. 5A, lower). Control MEL cells and Prmt1 knockdown cells were fractionated in cytoplasmic, cytoskeletal/nucleoplasmic, chromatin-associated, and nuclear matrix-associated proteins. An antibody directed against the C terminus of Prmt1 showed that Prmt1 localized to the cytoplasm and the soluble nuclear fraction (Fig. 5A). In contrast, Fop was found exclusively in the nucleus, with the majority of the protein being tightly associated with chromatin. Reducing

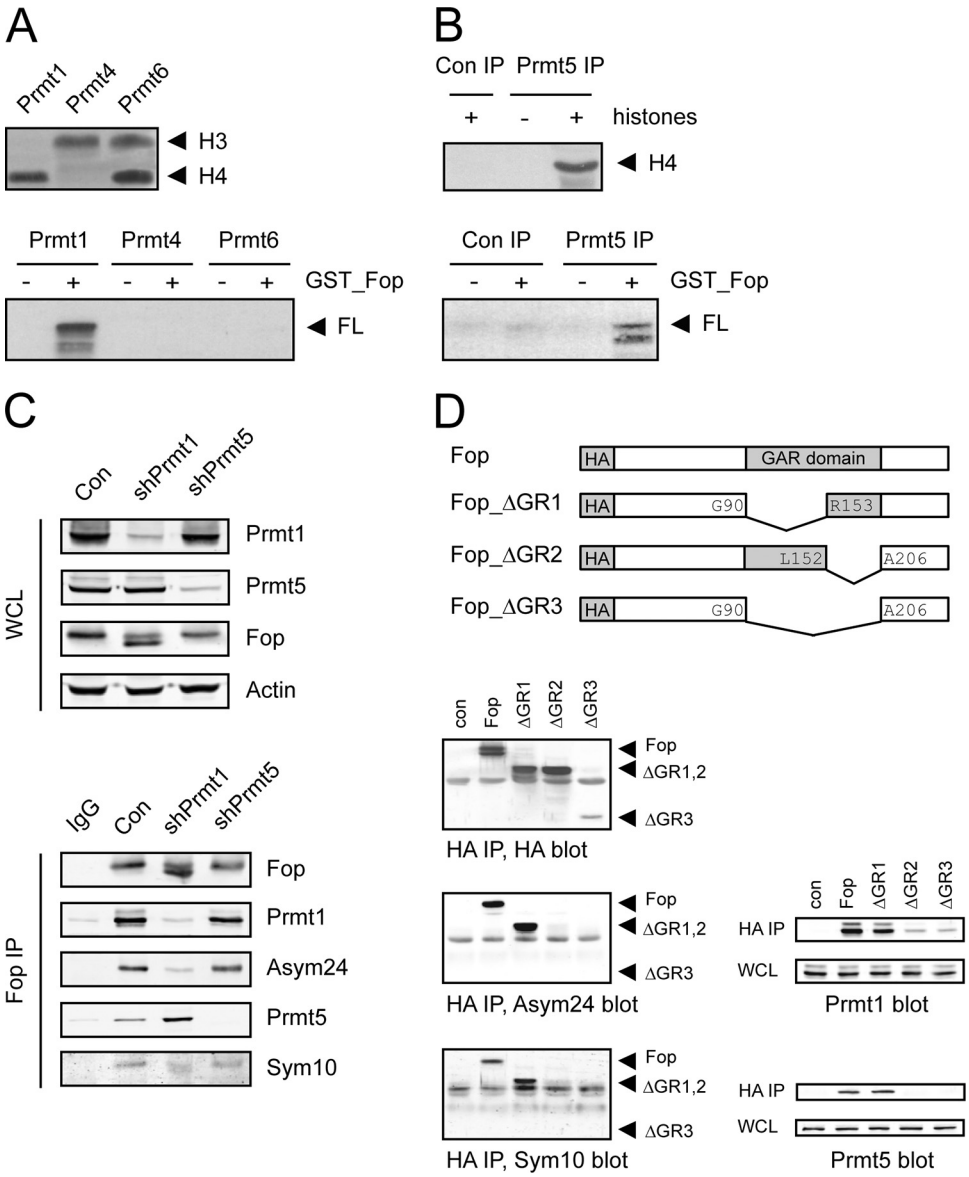

FIG. 4. Fop is a target for type I and type II Prmts. (A) GST_Fop_L was used as a substrate in an in vitro methylation assay using three type I GST_Prmts. Core histones were used as a positive control. Prmt1 is the only type I enzyme that can methylate full-length (FL) protein. (B) GST_Fop_L was used as a substrate in an in vitro methylation assay using immunoprecipitated Prmt5. (C) MEL cells were infected with control lentivirus (Con) or lentivirus expressing an shRNA against Prmt1 (Prmt1 kd). Whole-cell lysates (WCL; upper) were tested for Prmt1, Prmt5, and Fop. Staining for actin served as a control for equal loading. Fop was precipitated (IP; lower) and tested for binding to Prmt1 and Prmt5 and for asymmetric (Asym24) and symmetric DMA residues (Sym10). (D) HA_Fop constructs lacking GAR sequences were tested for methylation and Prmt1 and Prmt5 binding.

the level of Prmt1 resulted in hypomethylated Fop but did not change its distribution pattern. This is consistent with the confocal data and shows that the association of Fop with chromatin does not depend on its asymmetrical methylation (Fig. 5A).

In light of their copurification (Fig. 1, 3, and 4) and colocalization (Fig. 5A), it is surprising that Prmt1 and Fop localize to different cellular compartments after biochemical fractionation (Fig. 5B). To investigate this further, we performed the live imaging of Fop and Prmt1 N-terminally tagged with GFP and Cherry, respectively. We first confirmed that Gfp_Fop and Cherry_Prmt1 still interact by coimmunoprecipitation experiments (not shown). We then coexpressed the proteins stably in U2OS cells. We selected clones with low expression levels of both proteins. Western blot analysis showed that Cherry_Prmt1 was expressed at approximately 25% of the endogenous Prmt1 level (not shown). In fractionation experiments, Gfp_Fop was distributed similarly to HA_Fop in MEL cells (not shown). The localization of Gfp_Fop was strictly nuclear, with a punctate/speckle-like distribution in areas with low levels of DAPI, similarly to endogenous and HA-tagged Fop in MEL cells (Fig. 2C and 5A, respectively). Time-lapse imaging shows that Gfp_Fop is completely released from condensed chromosomes

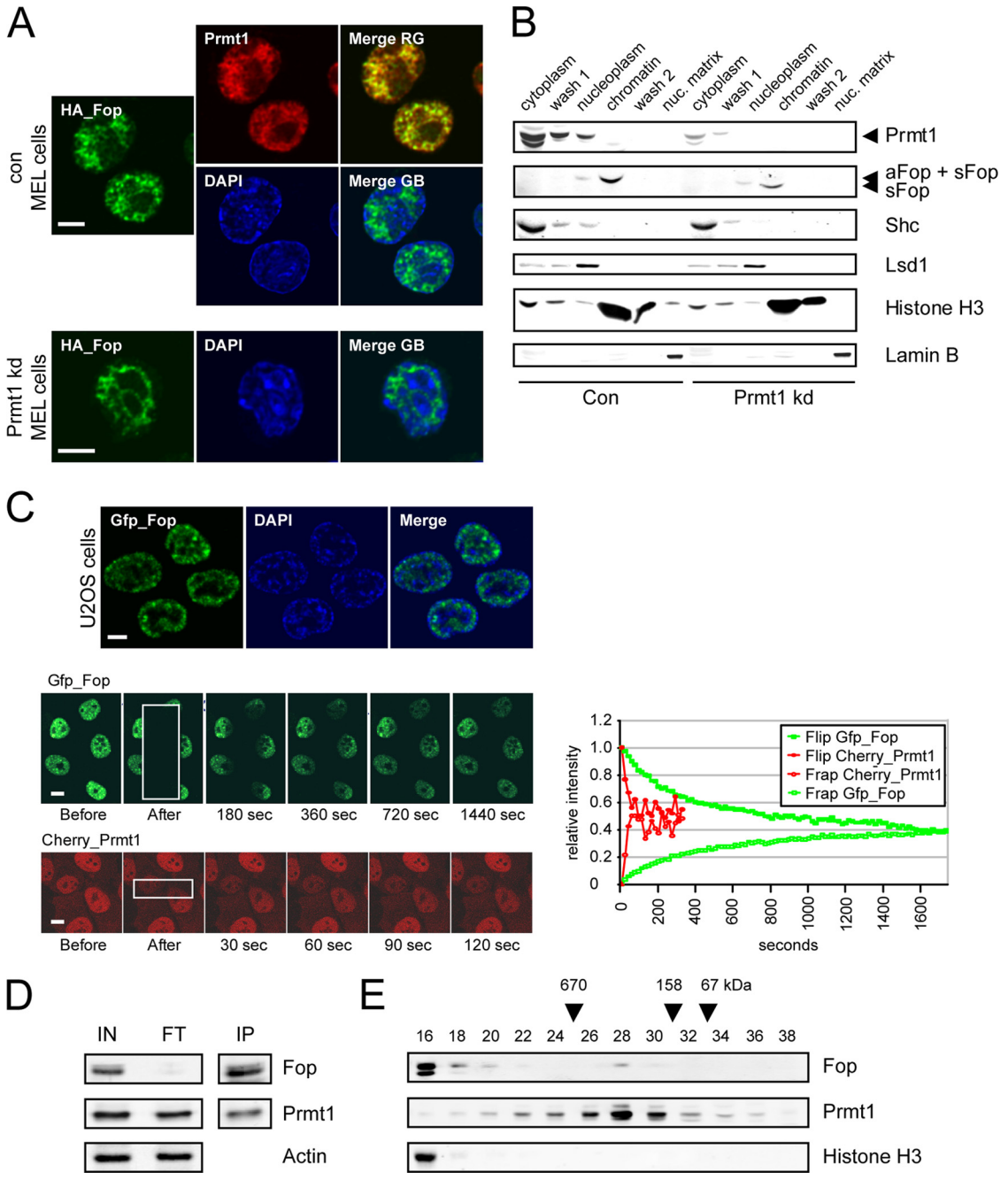

FIG. 5. Fop stably interacts with chromatin. (A) Confocal slices indicate that HA_Fop (immunofluorescence; cytospins of MEL cells) and Gfp_Fop (living U2OS cells) localize to regions in the nucleus with low levels of DAPI and display a granulated/speckle-like distribution. Nuclear Prmt1 has a more diffuse distribution but also localizes to regions that have low levels of DAPI or are euchromatic. The distribution of HA_Fop is not changed in cells with reduced Prmt1 expression (Prmt1 kd). Scale bars, 5 μm. Image stacks were deconvolved and corrected for chromatic shift. RG, red and green signals; GB, green and blue signals. (B) Cellular fractionation of control (Con) and Prmt1 knockdown (Prmt1 kd) MEL cells expressing HA_Fop. Cytoplasmic, nucleoplasmic, chromatin, and nuclear (nuc.) matrix fractions were tested for Prmt1 and Fop. Prmt1 localizes to the cytoplasm and nucleoplasm, while Fop (asymmetrically [aFop] and/or symmetrically methylated [sFop]) is associated with chromatin. Shc, LSD1, histone H3, and lamin B served as controls for individual fractions. (C) In vivo mobility of Fop and Prmt1 was determined by combined FRAP/FLIP. A new equilibrium in the distribution of Cherry_Prmt1 was reached within 30 s, which is consistent with the diffusion characteristics of a macromolecular complex of less than 1 MDa. Gfp_Fop is highly immobile, with complete redistribution taking more than 25 min. Scale bars, 10 μm. (D) The level of Prmt1 was determined in the input (IN) and flowthrough (FT) of Fop-depleted nuclear extracts of MEL cells (left). (E) Size fractionation profiles of Fop and Prmt1 in MEL nuclear extracts. Histone H3 staining served as a control for chromatin-containing fractions. Molecular mass markers are indicated at the top.

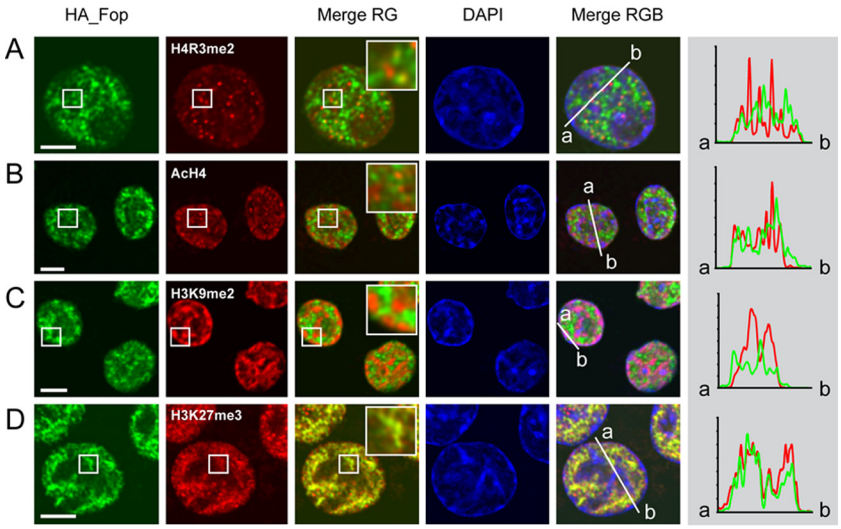

FIG. 6. HA_Fop colocalizes partially with H3K27me3. (A to D) Colocalization of HA_Fop was studied in cytospins of MEL cells labeled for immunofluorescence with anti-HA (green) and the antibodies indicated (red). Histograms represent quantified intensity profiles from points a to b (the *y* axis indicates pixel intensity). Partial colocalization is observed with H3K27me3, a mark for facultative heterochromatin. Scale bars, 5 μm. Image stacks were deconvolved and corrected for chromatic shift. RG, red and green signals; RGB, red, green, and blue signals.

during mitosis and relocates in ~1 h after cell division (not shown). To determine the mobility of Fop and Prmt1 in vivo, we combined FRAP and FLIP experiments. Half of a nucleus was bleached, and the recovery of fluorescence subsequently was monitored in the bleached part of the nucleus for 1,800 s. At the same time, the fluorescence loss in the unbleached part of the nucleus was monitored until a new equilibrium in fluorescence distribution was reached between the bleached and the unbleached regions. This experiment revealed that Cherry_Prmt1 behaves as a soluble protein with the diffusion characteristics of an oligomeric complex (Fig. 5C), which is consistent with previous data on Gfp_Prmt1 (18). In contrast, Gfp_Fop is a highly immobile protein with a diffusion rate more than 50 times slower than that of Prmt1 (Fig. 5C). Although the N-terminal tags may influence the behavior of both fusion proteins, these experiments indicate that Fop is not a component of a stable Prmt1-holoenzyme complex in vivo (17). To determine the fraction of Prmt1 that is associated with Fop, nuclear extracts were immunodepleted for endogenous Fop. Figure 5D shows that the complete depletion of Fop has a marginal effect on the amount of Prmt1 in the supernatant, indicating that only a small fraction of Prmt1 is bound to Fop. This is further demonstrated by size fractionation experiments: the majority of Fop and Prmt1 do not elute in the same fractions (Fig. 5E).

Fop colocalizes with facultative heterochromatin. The localization of Fop was further characterized by coimmunostaining with antibodies against different histone modifications. First, we used an antibody that was raised against asymmetrically dimethylated R3 of histone H4 (H4R3me2as). This methylation is performed by Prmt1 and is a critical step in subsequent transcription activation events, including histone acetylation (20, 43). Staining for H4R3me2as, as well as for acetylated H4 (acH4), a mark for active genes, revealed distinctive fluorescent spots (Fig. 6A, B). Although these spots resided within euchromatic (i.e., low levels of DAPI) regions of the nucleus, they showed only minor colocalization with Fop. H3K9me2 has been implicated in heterochromatin formation and gene silencing (5) and marks condensed DNA. As expected, H3K9me2 staining showed an almost complete overlap with these heterochromatic regions (Fig. 6C). Fop was excluded from those regions that are positive for H3K9me2 staining, showing that Fop is not localized to condensed DNA, which is in line with the observation that Gfp_Fop detaches from mitotic chromosomes. The methylation of K27 of histone H3 (H3K27me3) creates binding sites for the polycomb repressive complex 1 (29) and therefore is a mark for facultative heterochromatin. Staining with an antibody that specifically recognized H3K27me3 identified bright spots and a more diffuse staining throughout the regions with low levels of DAPI (Fig. 6D). The diffuse signal showed a striking colocalization with Fop, while only a minority of the bright spots was found to be double positive for Fop and H3K27me3. We conclude that at this level of resolution, Fop is associated mainly with facultative heterochromatin in vivo.

Fop is critical for estrogen-dependent gene activation. The observations that Fop is tightly bound to chromatin after biochemical fractionation and colocalizes with facultative heterochromatin in vivo suggest that it is involved in transcriptional regulation. The significance of Prmt1 in transcriptional regulation has been demonstrated most vividly in the model of nuclear hormone signaling. The recruitment of Prmt1 and the subsequent methylation of H4R3 are critical events in the ER-regulated activation of the *pS2* gene (*TFF1*, encoding trefoil factor 1). Since the molecular events leading to the activation of this gene have been described in detail (27, 28), we studied the functional importance of Fop in the E2 induction of pS2 expression in MCF7 cells, a human E2-responsive breast cancer cell line. Cells were seeded in hormone-free medium and subsequently transfected with siRNAs against GFP (siGFP), Prmt1 (siPrmt1), and siFop, respectively. Western blot analysis showed the suppression of endogenous Prmt1 and Fop 48 h after siRNA treatment (Fig. 7A). Furthermore,

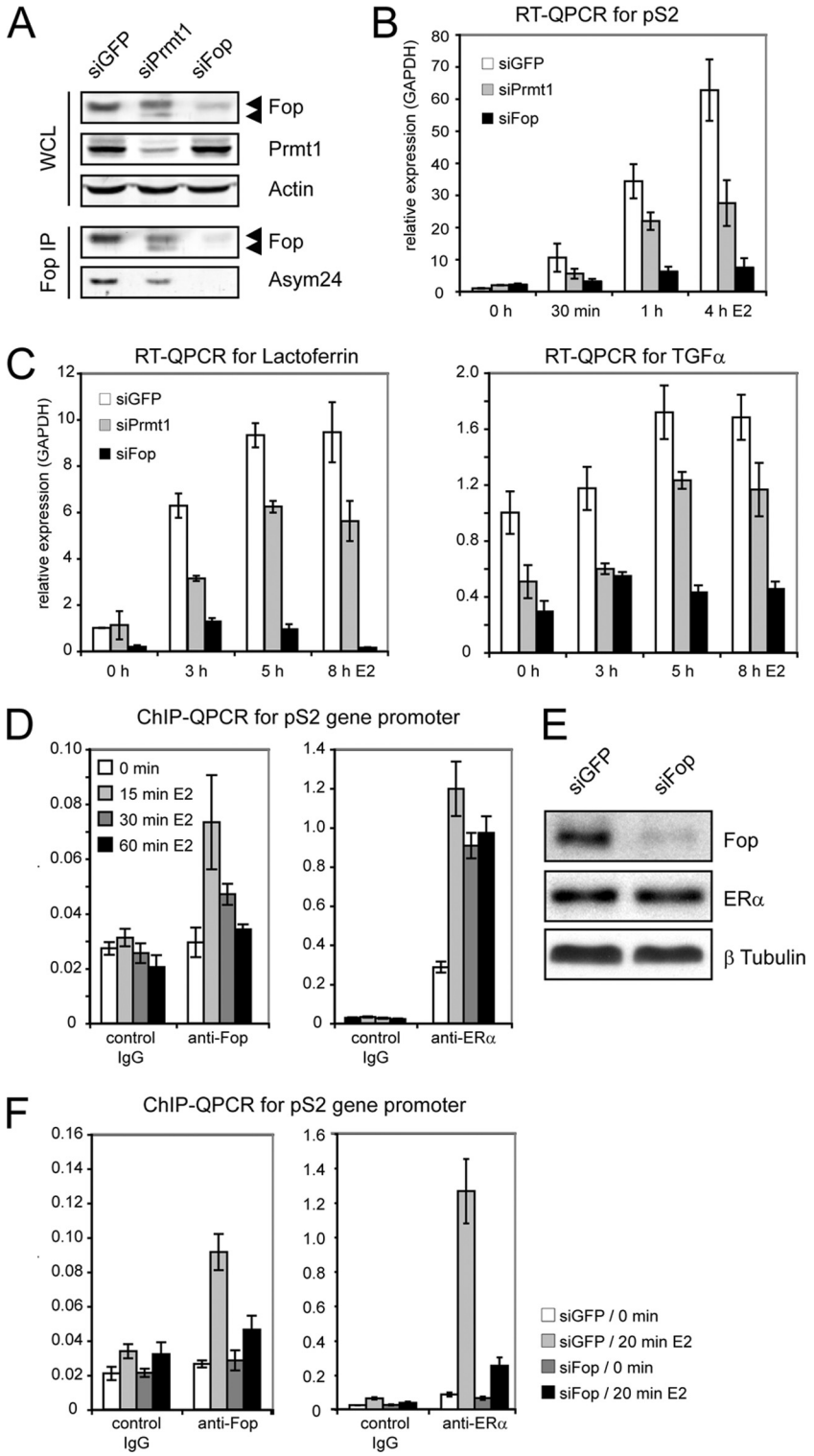

FIG. 7. Fop is critical for E2-dependent gene activation. (A to F) MCF7 cells were hormone starved and treated with siRNAs as indicated. (A) Whole-cell lysates (WCL) and IPs were stained by Western blotting with the indicated antibodies. (B and C) MCF7 cells were induced with E2 for the times indicated. Total RNA was analyzed by RT-QPCR using primers for pS2, lactoferrin, and TGF-α. (D) MCF7 cells were treated for 0, 15, 30, and 60 min with E2. ChIP reactions was performed with the indicated antibodies and examined by QPCR for the presence of proximal pS2 promoter fragments. (E) Whole-cell lysates were analyzed by Western blotting with the indicated antibodies. (F) MCF7 cells were treated with siRNAs against GFP or Fop for 48 h, followed by E2 induction. ChIP-QPCR was performed as described for panel D.

the reduction of Prmt1 expression resulted in the partial hypomethylation of Fop, as demonstrated by the appearance of a faster-migrating species of Fop and reduced staining for Asym24 (Fig. 7A). To analyze ER-regulated transcription, cells were induced with E2 for various times and RNA was isolated. As described previously (47), RT-QPCR revealed that the E2-induced transcriptional activity of endogenous pS2 was reduced upon siPrmt1 transfection compared to that of siGFP transfection (Fig. 7B). Interestingly, the reduction of the endogenous Fop level had a more dramatic inhibitory effect on pS2 induction. Similar results were obtained with two siRNAs that target different regions of the Fop mRNA (not shown). We next tested the effect of reduced Fop levels on the E2-induced transcription of *Lactoferrin* and *TGFα*, two other Prmt1-dependent E2-inducible genes. Consistently with the observations for the *pS2* gene, the E2-induced transcriptional activity of these genes was diminished upon siPrmt1 transfection and was almost absent after siFop transfection (Fig. 7C). Furthermore, reduced Fop levels resulted in lower preinduction transcript levels of these genes. To investigate whether the transcriptional effect of Fop correlates with the binding of Fop to the *pS2* promoter, we performed ChIP analysis following E2 induction. Chromatin was precipitated with antibodies against Fop, ERα, and control IgG and analyzed by PCR for the presence of *pS2* promoter fragments, including the ER element. Promoter occupancy by Fop was not detected in uninduced cells, but in E2-treated cells a transient interaction was observed with a peak at 15 min postinduction (Fig. 7D, left). The promoter occupancy of ERα also increased 15 min after E2 addition and remained constant during the measured period (Fig. 7D, right). We next tested whether Fop depletion affected the binding of ERα to the *pS2* promoter. MCF7 cells were transfected with siGFP and siFop. Two days later, cells were induced with E2 for 20 min and analyzed by ChIP using antibodies against Fop, ERα, and control IgG. As expected, reduced Fop levels (Fig. 7E) resulted in reduced Fop binding to the *pS2* promoter (Fig. 7F, left). Although transfection with siFop did not change the protein level of ERα (Fig. 7E), a dramatic reduction in promoter occupancy by ERα was observed (Fig. 7F, right). Taken together, these data show that Fop is required for the E2-inducible expression of the ERα target genes investigated and for the binding of ERα to the *pS2* promoter region.

DISCUSSION

Here, we identified a novel protein, Fop, in an unbiased proteomics screen for Prmt1-interacting proteins. All identified Prmt1-associated factors, including Fop, contain glycine-arginine-rich regions, a sequence with high affinity for Prmt1 (51). Proteins that have been described to bind to Prmt1 with domains other than GARs, such as Btg1 and Btg2, Nip45, or Usf1, were not identified. There are several possible explanations: the proteins are not expressed in MEL cells or are expressed only during a short period of the cell cycle (as is the case for Btg1 and Btg2 [4, 41]), the interactions are transient or unstable, or GAR-containing proteins compete efficiently for Prmt1 binding during the isolation. In this study, we showed that Fop and Prmt1 are strongly associated in coimmunoprecipitation assays. However, immunodepletion, size fractionation, and FRAP/FLIP experiments show that both in vitro and in vivo the majority of Prmt1 is not associated with Fop. We therefore conclude that Fop is not a part of the Prmt1 holoenzyme complex. The remaining Prmt1-associated factors identified in our screen are RNA-binding proteins and most likely represent Prmt1 targets rather than structural components of the 250- to 400-kDa Prmt1 complex. Collectively, our results favor the hypothesis that the Prmt1 holoenzyme is composed of Prmt1 multimers (24, 48, 51).

Fop is a novel target of protein arginine methyltransferases. Structurally, Fop can be divided in three regions: a central GAR domain flanked by N- and C-terminal parts that do not contain any known functional motifs. Nevertheless, the fact that Fop is highly conserved in all vertebrates suggests that it is an important protein for this subphylum and that all three regions harbor critical information for Fop function. Possibly, Fop acts as a scaffold protein with three interaction domains.

Type I methylation by Prmt1 and Prmt4 serves as a general marker for active transcription, while type II methylation by Prmt5 and Prmt7 is associated with transcriptional repression. From this perspective, it is highly interesting that Fop also is symmetrically methylated by Prmt5 in vivo. In the absence of Prmt1, Fop no longer is asymmetrically methylated. Still, its distribution pattern and chromatin association are not affected. Since arginine methylation is known to regulate protein-protein interactions, this suggests that Fop recruits proteins to chromatin in a methylation-dependent manner.

Western blot analysis revealed an unprecedented mobility shift of Fop in cells with reduced Prmt1 levels, strongly suggesting that multiple arginines are methylated by this enzyme. However, the mapping of the target arginines is compromised by the fact that the GAR domain contains 26 arginines that potentially are methylated, as they are flanked by a glycine residue. Our results indicate that the majority of target arginines are located in the C-terminal half of the GAR domain. However, the number and position of target arginines, as well as the dynamics of their methylation status, are unclear. The observation that both the slower-migrating and the faster-migrating species of Fop lacking aDMA are recognized by the SYM10 antibody opens the possibility that a single Fop molecule contains aDMA and sDMA at the same time.

Fop is associated with chromatin and required for E2-dependent gene expression. Immunofluorescence and GFP fusion studies reveal that Fop mainly associates with noncondensed (DAPI- and H3K9me2-negative) chromatin, while it is released from mitotic chromosomes. It is possible that Fop binds directly to DNA, as it shares some characteristics with histones: (i) it is a highly basic protein, with an estimated pI of 12.2, and (ii) its association with chromatin is extremely stable. The localization of Fop shows a striking colocalization with H3K27me3, indicating that Fop is associated with facultative heterochromatin. This raises the possibility that Fop is involved in the regulation of genes responding to environmental and developmental cues, such as growth factors and hormones. To test this directly, we analyzed the role of Fop in the induction of the *pS2* gene by E2. Ligand-bound ERα induces the recruitment of coactivators and specific histone modifications at the *pS2* promoter (28). While Prmt1 methylates cytoplasmic ERα to control the extranuclear function of the receptor, the recruitment of Prmt1 is a critical event for H4R3 methylation

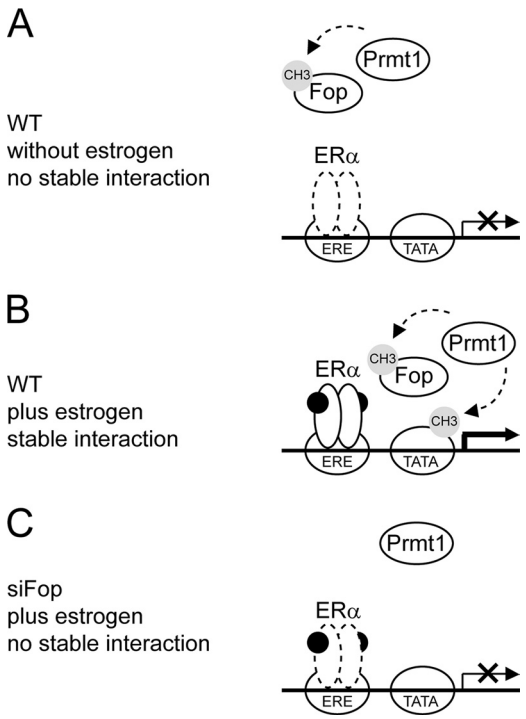

FIG. 8. Model for Fop function in ER-regulated gene expression. (A) In the absence of hormone, ERα is weakly bound to the promoter. WT, wild type. (B) Upon ligand binding, the interaction between ERα and its target sequences is stabilized, while Fop and Prmt1 are recruited. Prmt1 methylates H4R3 and Fop, although the latter also may take place elsewhere. These events are critical for high transcription levels. (C) Reduced Fop levels impair a stable interaction of ERα and the promoter, resulting in a block of transcription. ERE, ER element.

and subsequent histone acetylation and the binding of the basal transcription machinery to the *pS2* promoter (23, 28, 47). Our ChIP data indicate that Fop is not present at the proximal promoter of the *pS2* gene in uninduced MCF7 cells, while it is recruited rapidly after E2 induction. Fop recruitment peaks after 15 min, coinciding with the recruitment of Prmt1 and the initiation of the first transcription cycle of the *pS2* gene. Remarkably, reduced Fop levels have a much stronger inhibiting effect on the induction of the *pS2*, *Lactoferrin*, and *TGFα* genes compared to those observed after Prmt1 depletion (Fig. 7) (47). Furthermore, Fop depletion results in an almost complete block of E2-induced promoter occupancy by ERα. These results indicate a central role for Fop in the stable recruitment of ERα to the *pS2* promoter. Since promoter occupancy by ERα in uninduced cells remains very similar after Fop knockdown, it appears that the inefficient binding of unliganded ERα to the ER element of the *pS2* promoter is unchanged in the absence of Fop. As a result of the transient nature of the knockdown experiments in MCF7 cells, depletion for Prmt1 resulted in the partial hypomethylation of Fop (Fig. 7A). Therefore, we were not able to further study the role of Prmt1-dependent methylation of Fop in this context, as the knockdown level of Prmt1 was not sufficient to obtain completely nonmethylated Fop (Fig. 7B). Since we have no evidence that Fop and ERα interact directly in noninduced or E2-induced MCF7 cells, our data suggest a model where Fop recruitment is an early event that is critical for a stable interaction between ERα and its target sequences (Fig. 8). Alternatively, Fop could facilitate a chromatin environment that is permissive for ERα binding in uninduced cells. Future experiments have to clarify the exact role of Fop in transcription regulation, as well as the significance of its methylation status in this process.

ACKNOWLEDGMENTS

We thank Karel Bezstarosti and Silvia Hoeboer for technical assistance.

This work was supported by the Landsteiner Foundation for Blood Transfusion Research (LSBR), the Dutch Scientific Organization (NWO), the Centre for Biomedical Genetics (CBG), The Netherlands Genomics Initiative (NGI), the Deutsche Forschungsgemeinschaft (DFG), and the European Union FP6 EUtracc consortium.

REFERENCES

1. **An, W., J. Kim, and R. G. Roeder.** 2004. Ordered cooperative functions of PRMT1, p300, and CARM1 in transcriptional activation by p53. Cell **117:** 735–748.
2. **Andrews, N. C., and D. V. Faller.** 1991. A rapid micropreparation technique for extraction of DNA-binding proteins from limiting numbers of mammalian cells. Nucleic Acids Res. **19:**2499.
3. **Bajpe, P. K., J. A. van der Knaap, J. A. Demmers, K. Bezstarosti, A. Bassett, H. M. van Beusekom, A. A. Travers, and C. P. Verrijzer.** 2007. Deubiquitylating enzyme UBP64 controls cell fate through stabilization of the transcriptional repressor Tramtrack. Mol. Cell. Biol. **28:**1606–1615.
4. **Bakker, W. J., M. Blazquez-Domingo, A. Kolbus, J. Besooyen, P. Steinlein, H. Beug, P. J. Coffer, B. Lowenberg, M. von Lindern, and T. B. van Dijk.** 2004. FoxO3a regulates erythroid differentiation and induces BTG1, an activator of protein arginine methyl transferase 1. J. Cell Biol. **164:**175–184.
5. **Bannister, A. J., P. Zegerman, J. F. Partridge, E. A. Miska, J. O. Thomas, R. C. Allshire, and T. Kouzarides.** 2001. Selective recognition of methylated lysine 9 on histone H3 by the HP1 chromo domain. Nature **410:**120–124.
6. **Bedford, M. T., and S. G. Clarke.** 2009. Protein arginine methylation in mammals: who, what, and why. Mol. Cell **33:**1–13.
7. **Bedford, M. T., A. Frankel, M. B. Yaffe, S. Clarke, P. Leder, and S. Richard.** 2000. Arginine methylation inhibits the binding of proline-rich ligands to Src homology 3, but not WW, domains. J. Biol. Chem. **275:**16030–16036.
8. **Boffa, L. C., J. Karn, G. Vidali, and V. G. Allfrey.** 1977. Distribution of NG, NG,-dimethylarginine in nuclear protein fractions. Biochem. Biophys. Res. Commun. **74:**969–976.
9. **Boisvert, F. M., J. Cote, M. C. Boulanger, P. Cleroux, F. Bachand, C. Autexier, and S. Richard.** 2002. Symmetrical dimethylarginine methylation is required for the localization of SMN in Cajal bodies and pre-mRNA splicing. J. Cell Biol. **159:**957–969.
10. **Boisvert, F. M., J. Cote, M. C. Boulanger, and S. Richard.** 2003. A proteomic analysis of arginine-methylated protein complexes. Mol. Cell Proteomics **2:**1319–1330.
11. **Brummelkamp, T. R., R. Bernards, and R. Agami.** 2002. A system for stable expression of short interfering RNAs in mammalian cells. Science **296:**550–553.
12. **de Boer, E., P. Rodriguez, E. Bonte, J. Krijgsveld, E. Katsantoni, A. Heck, F. Grosveld, and J. Strouboulis.** 2003. Efficient biotinylation and single-step purification of tagged transcription factors in mammalian cells and transgenic mice. Proc. Natl. Acad. Sci. USA **100:**7480–7485.
13. **Duong, F. H., V. Christen, J. M. Berke, S. H. Penna, D. Moradpour, and M. H. Heim.** 2005. Upregulation of protein phosphatase 2Ac by hepatitis C virus modulates NS3 helicase activity through inhibition of protein arginine methyltransferase 1. J. Virol. **79:**15342–15350.
14. **Essers, J., A. B. Houtsmuller, and R. Kanaar.** 2006. Analysis of DNA recombination and repair proteins in living cells by photobleaching microscopy. Methods Enzymol. **408:**463–485.
15. **Fackelmayer, F. O.** 2005. Protein arginine methyltransferases: guardians of the Arg? Trends Biochem. Sci. **30:**666–671.
16. **Follenzi, A., G. Sabatino, A. Lombardo, C. Boccaccio, and L. Naldini.** 2002. Efficient gene delivery and targeted expression to hepatocytes in vivo by improved lentiviral vectors. Hum. Gene Ther. **13:**243–260.
17. **Goulet, I., G. Gauvin, S. Boisvenue, and J. Cote.** 2007. Alternative splicing yields protein arginine methyltransferase 1 isoforms with distinct activity, substrate specificity, and subcellular localization. J. Biol. Chem. **282:**33009–33021.
18. **Herrmann, F., J. Lee, M. T. Bedford, and F. O. Fackelmayer.** 2005. Dynamics of human protein arginine methyltransferase 1 (PRMT1) in vivo. J. Biol. Chem. **280:**38005–38010.
19. **Huang, S., X. Li, T. M. Yusufzai, Y. Qiu, and G. Felsenfeld.** 2007. USF1 recruits histone modification complexes and is critical for maintenance of a chromatin barrier. Mol. Cell. Biol. **27:**7991–8002.

20. **Huang, S., M. Litt, and G. Felsenfeld.** 2005. Methylation of histone H4 by arginine methyltransferase PRMT1 is essential in vivo for many subsequent histone modifications. Genes Dev. **19:**1885–1893.
21. **Hyllus, D., C. Stein, K. Schnabel, E. Schiltz, A. Imhof, Y. Dou, J. Hsieh, and U. M. Bauer.** 2007. PRMT6-mediated methylation of R2 in histone H3 antagonizes H3 K4 trimethylation. Genes Dev. **21:**3369–3380.
22. **Kaufman, R. J., M. V. Davies, V. K. Pathak, and J. W. Hershey.** 1989. The phosphorylation state of eucaryotic initiation factor 2 alters translational efficiency of specific mRNAs. Mol. Cell. Biol. **9:**946–958.
23. **Le Romancer, M., I. Treilleux, N. Leconte, Y. Robin-Lespinasse, S. Sentis, K. Bouchekioua-Bouzaghou, S. Goddard, S. Gobert-Gosse, and L. Corbo.** 2008. Regulation of estrogen rapid signaling through arginine methylation by PRMT1. Mol. Cell **31:**212–221.
24. **Lim, Y., Y. H. Kwon, N. H. Won, B. H. Min, I. S. Park, W. K. Paik, and S. Kim.** 2005. Multimerization of expressed protein-arginine methyltransferases during the growth and differentiation of rat liver. Biochim. Biophys. Acta **1723:**240–247.
25. **Lin, W. J., J. D. Gary, M. C. Yang, S. Clarke, and H. R. Herschman.** 1996. The mammalian immediate-early TIS21 protein and the leukemia-associated BTG1 protein interact with a protein-arginine N-methyltransferase. J. Biol. Chem. **271:**15034–15044.
26. **Liu, Q., and G. Dreyfuss.** 1995. In vivo and in vitro arginine methylation of RNA-binding proteins. Mol. Cell. Biol. **15:**2800–2808.
27. **Métivier, R., G. Penot, M. R. Hubner, G. Reid, H. Brand, M. Kos, and F. Gannon.** 2003. Estrogen receptor-alpha directs ordered, cyclical, and combinatorial recruitment of cofactors on a natural target promoter. Cell **115:** 751–763.
28. **Métivier, R., G. Reid, and F. Gannon.** 2006. Transcription in four dimensions: nuclear receptor-directed initiation of gene expression. EMBO Rep. **7:**161–167.
29. **Min, J., Y. Zhang, and R. M. Xu.** 2003. Structural basis for specific binding of polycomb chromodomain to histone H3 methylated at Lys 27. Genes Dev. **17:**1823–1828.
30. **Mowen, K. A., B. T. Schurter, J. W. Fathman, M. David, and L. H. Glimcher.** 2004. Arginine methylation of NIP45 modulates cytokine gene expression in effector T lymphocytes. Mol. Cell **15:**559–571.
31. **Nair, S. S., S. K. Mishra, Z. Yang, S. Balasenthil, R. Kumar, and R. K. Vadlamudi.** 2004. Potential role of a novel transcriptional coactivator PELP1 in histone H1 displacement in cancer cells. Cancer Res. **64:**6416–6423.
32. **Needham, M., C. Gooding, K. Hudson, M. Antoniou, F. Grosveld, and M. Hollis.** 1992. LCR/MEL: a versatile system for high-level expression of heterologous proteins in erythroid cells. Nucleic Acids Res. **20:**997–1003.
33. **Ong, S. E., G. Mittler, and M. Mann.** 2004. Identifying and quantifying in vivo methylation sites by heavy methyl SILAC. Nat. Methods **1:**119–126.
34. **Pahlich, S., R. P. Zakaryan, and H. Gehring.** 2006. Protein arginine methylation: cellular functions and methods of analysis. Biochim. Biophys. Acta **1764:**1890–1903.
35. **Pal, S., R. A. Baiocchi, J. C. Byrd, M. R. Grever, S. T. Jacob, and S. Sif.** 2007. Low levels of miR-92b/96 induce PRMT5 translation and H3R8/H4R3 methylation in mantle cell lymphoma. EMBO J. **26:**3558–3569.
36. **Pal, S., and S. Sif.** 2007. Interplay between chromatin remodelers and protein arginine methyltransferases. J. Cell Physiol. **213:**306–315.
37. **Pasqualini, C., D. Guivarc'h, J. V. Barnier, B. Guibert, J. D. Vincent, and P. Vernier.** 2001. Differential subcellular distribution and transcriptional activity of sigmaE3, sigmaE4, and sigmaE3-4 isoforms of the rat estrogen receptor-alpha. Mol. Endocrinol. **15:**894–908.
38. **Pawlak, M. R., C. A. Scherer, J. Chen, M. J. Roshon, and H. E. Ruley.** 2000. Arginine *N*-methyltransferase 1 is required for early postimplantation mouse development, but cells deficient in the enzyme are viable. Mol. Cell. Biol. **20:**4859–4869.
39. **Rezai-Zadeh, N., X. Zhang, F. Namour, G. Fejer, Y. D. Wen, Y. L. Yao, I. Gyory, K. Wright, and E. Seto.** 2003. Targeted recruitment of a histone H4-specific methyltransferase by the transcription factor YY1. Genes Dev. **17:**1019–1029.
40. **Robin-Lespinasse, Y., S. Sentis, C. Kolytcheff, M. C. Rostan, L. Corbo, and M. Le Romancer.** 2007. hCAF1, a new regulator of PRMT1-dependent arginine methylation. J. Cell Sci. **120:**638–647.
41. **Rouault, J. P., R. Rimokh, C. Tessa, G. Paranhos, M. Ffrench, L. Duret, M. Garoccio, D. Germain, J. Samarut, and J. P. Magaud.** 1992. BTG1, a member of a new family of antiproliferative genes. EMBO J. **11:**1663–1670.
42. **Shen, E. C., M. F. Henry, V. H. Weiss, S. R. Valentini, P. A. Silver, and M. S. Lee.** 1998. Arginine methylation facilitates the nuclear export of hnRNP proteins. Genes Dev. **12:**679–691.
43. **Strahl, B. D., S. D. Briggs, C. J. Brame, J. A. Caldwell, S. S. Koh, H. Ma, R. G. Cook, J. Shabanowitz, D. F. Hunt, M. R. Stallcup, and C. D. Allis.** 2001. Methylation of histone H4 at arginine 3 occurs in vivo and is mediated by the nuclear receptor coactivator PRMT1. Curr. Biol. **11:**996–1000.
44. **Tang, J., J. D. Gary, S. Clarke, and H. R. Herschman.** 1998. PRMT 3, a type I protein arginine N-methyltransferase that differs from PRMT1 in its oligomerization, subcellular localization, substrate specificity, and regulation. J. Biol. Chem. **273:**16935–16945.
45. **van Dijk, T. B., E. van Den Akker, M. P. Amelsvoort, H. Mano, B. Lowenberg, and M. von Lindern.** 2000. Stem cell factor induces phosphatidylinositol 3′-kinase-dependent Lyn/Tec/Dok-1 complex formation in hematopoietic cells. Blood **96:**3406–3413.
46. **Wada, K., K. Inoue, and M. Hagiwara.** 2002. Identification of methylated proteins by protein arginine N-methyltransferase 1, PRMT1, with a new expression cloning strategy. Biochim. Biophys. Acta **1591:**1–10.
47. **Wagner, S., S. Weber, M. A. Kleinschmidt, K. Nagata, and U. M. Bauer.** 2006. SET-mediated promoter hypoacetylation is a prerequisite for coactivation of the estrogen-responsive pS2 gene by PRMT1. J. Biol. Chem. **281:**27242–27250.
48. **Wang, H., Z. Q. Huang, L. Xia, Q. Feng, H. Erdjument-Bromage, B. D. Strahl, S. D. Briggs, C. D. Allis, J. Wong, P. Tempst, and Y. Zhang.** 2001. Methylation of histone H4 at arginine 3 facilitating transcriptional activation by nuclear hormone receptor. Science **293:**853–857.
49. **Xu, W., H. Chen, K. Du, H. Asahara, M. Tini, B. M. Emerson, M. Montminy, and R. M. Evans.** 2001. A transcriptional switch mediated by cofactor methylation. Science **294:**2507–2511.
50. **Yu, M. C., F. Bachand, A. E. McBride, S. Komili, J. M. Casolari, and P. A. Silver.** 2004. Arginine methyltransferase affects interactions and recruitment of mRNA processing and export factors. Genes Dev. **18:**2024–2035.
51. **Zhang, X., and X. Cheng.** 2003. Structure of the predominant protein arginine methyltransferase PRMT1 and analysis of its binding to substrate peptides. Structure **11:**509–520.
52. **Zufferey, R., D. Nagy, R. J. Mandel, L. Naldini, and D. Trono.** 1997. Multiply attenuated lentiviral vector achieves efficient gene delivery in vivo. Nat. Biotechnol. **15:**871–875.